Current Research in Toxicology 7 (2024) 100196

Contents lists available at ScienceDirect

Current Research in Toxicology

journal homepage: www.journals.elsevier.com/current-research-in-toxicology

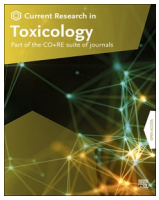

Research Paper

Tocotrienol suppresses colitis-associated cancer progression through TLR4 signaling in a mouse model of colorectal cancer

Qian Li [a,1], Shujing Zhang [b,c,1], Qinghong Zhou [b,c], Chenxi Gu [d], Yinghua Liu [b,c], Jing Zhang [b,c], Jingshu Zhang [e,*]

[a] School of Public Health, Qilu Medical University, Shandong 255300, China
[b] Department of Toxicology, Tianjin Centers for Disease Control and Prevention, Tianjin 300011, China
[c] NHC Specialty Laboratory of Food Safety Risk Assessment and Standard Development, Tianjin 300011, China
[d] Disease Prevention and Control Center of Binhu District, Wuxi City, Jiangsu 214100, China
[e] School of Public Health, Nanjing Medical University, Nanjing 211166, China

ARTICLE INFO

Keywords:
Annatto-tocotrienol
Colorectal cancer
TLR4 signaling
Cytokines

ABSTRACT

This study aimed to evaluate the preventive efficacy of tocotrienol in inhibiting the nuclear factor-kappa B (NF-κB) mediated inflammation pathways in colorectal cancer. We utilized the azoxymethane (AOM) and dextran sulfate sodium salt (DSS) to induce colitis-associated colorectal cancer (CAC) mice model. In generating a CAC model, mice were intraperitoneally injected with AOM at a concentration of 10 mg/kg body weight. Seven days after the AOM injection, mice drinking water containing 3 % DSS for 1 week, followed by a 2-week period of regular water. This cycle of DSS treatment (1-week 3 % DSS+2-week water) was repeated for two additional cycles. Mice were randomly divided into five groups (n = 20/group), including Blank group, Model group, three different dosages tocotrienol groups (Low dose group [50 mg/kg], Medium dose group [75 mg/kg], and High dose group [100 mg/kg]). The protective effects of tocotrienol were assessed using histological, flow cytometry, western blot and mouse Luminex assay. Compared with the blank group, expressions of toll-like receptor 4 (TLR4), myeloid differentiation protein 88 (MyD88), tumor necrosis factor receptor-associated factor 6 (TRAF-6), NF-κB, Interleukin (IL)-6 and tumor necrosis factor (TNF) −α were increased in model group, while IL-4 and IL-10 were decreased in model group ($P<0.05$). Tocotrienol prevented carcinogenesis and decreased the IL-6, TNF-α, MyD88, TLR4, TRAF-6 and NF-κB expression levels, compared with the model group ($P<0.05$). Compared with the model group, the expression of IL-10 was increased in medium dose group and high dose group ($P<0.05$). The protective effects of tocotrienol may be related to the inhibition of TLR4 /MyD88 /NF-κB mediated inflammatory signaling pathways. Therefore, the use of tocotrienol can improve the abnormal expression of cytokines in a mouse model of colorectal cancer and inhibit the occurrence and development of colorectal cancer.

1. Introduction

Colorectal cancer is a malignant tumor of the digestive system and is the second leading cause of cancer death and the third most common cancer globally. This malignancy induces estimated 1.9 million incidence cases and 0.9 million deaths worldwide (Bray et al., 2024). Colitis-associated cancer (CAC) is a subtype of colorectal cancer (CRC) associated with inflammatory bowel disease (IBD). Extensive evidence suggested that the micro-environment surrounding the intestinal epithelial cells in IBD patients can promote inflammation −associated epithelial cell damage, and thereby facilitate the occurrence and progression of CAC (Terzić et al., 2010; Hirano et al., 2020; Sharma et al., 2018). Currently, the main treatment approaches for colorectal cancer (CRC) are surgery and chemoradiotherapy. Nevertheless, these interventions have limited efficacy, resulting in a five-year relative survival rate of only about 15 % for patients with distant CRC (Siegel et al., 2022). Furthermore, chronic inflammation over an extended period is a notable risk factor for the onset of CRC.

To study the mechanisms and preventive measures of CAC, the azoxymethane (AOM)/dextran sulfate sodium (DSS) mouse model is

* Corresponding author at: Department of Toxicology, School of Public Health, Nanjing Medical University, Nanjing 211166, China.
E-mail address: Jingshuzh@njmu.edu.cn (J. Zhang).
[1] Both authors contributed equally to this work and should be considered co-first authors.

https://doi.org/10.1016/j.crtox.2024.100196
Received 14 March 2024; Received in revised form 20 September 2024; Accepted 20 September 2024
Available online 26 September 2024

predominantly used. This model is similar in histological and molecular characteristics to human CAC. Drinking water containing DSS can induce colitis in the mouse, and repeated exposure can induce colorectal cancer, although with low tumor incidence and a long modeling period (Tanaka et al., 2003; Suzuki et al., 2005). A single injection of AOM prior to DSS exposure has been shown to induce persistent damage and repair of the intestinal mucosal epithelium in mice, which shortens the modeling period and increases the tumorigenesis rate, and has been widely applied (Popivanova et al., 2008). Son et al. observed the effects of AOM/DSS treatment on tumorigenesis rates in different sexes of CD-1 (ICR) mice, compared the number and incidence of low-grade adenomas, high-grade adenomas, cancerous mucosal invasion, and cancerous submucosal invasion in colon tissue samples collected at different time points, and found that both the number and incidence of tumors in female mice were lower than those in male mice (Son et al., 2019). Therefore, we used the male CD-1 (ICR) mice to evaluate the preventative and therapeutic effects of tocotrienol on AOM/DSS induced CAC model in mice, as well as its regulatory effects on inflammatory pathways.

The Toll-like receptor 4/myeloid differentiation protein 88/nuclear factor κB (TLR4/MyD88/NF-κB) signaling pathway plays a crucial role in the progression of colitis to CAC (Pastille et al., 2021). TLR4 is a pattern recognition receptor for lipopolysaccharide (LPS) and participates in the inflammatory response by regulating the expression of adaptive immune-related proteins (Fukata et al., 2009). TLR4 can activate two signaling pathways, namely, a MyD88-dependent or MyD88-independent pathway. In a resting state, MyD88 forms a signaling complex with IL-1 receptor-associated kinase (IRAK) and TNF receptor-associated factor 6 (TRAF6). Following LPS stimulation, TLR4 activation leads to the phosphorylation of IRAK, and then TRAF6 is dissociated from the signaling complex (Li et al., 2019). TRAF 6 is a ubiquitin E3 ligase that acts as a adapter protein in TLRs signal pathways. TRAF6 promotes NF-κB signaling through K63 polyubiquitination of inhibitor of κB Kinase (IKK), leading to the activation of IKK. Inhibitor of κB (IκB) was phosphorylated by IKK and followed by proteasome-mediated degradation of IκB leading to the nuclear translocation of NF-κB and promoting the release of cytokines such as IL-1, IL-6, TNF-α, and IL-1β (Luan et al., 2014; Deng et al., 2000; Liu et al., 2018).The increased levels of TNF-α and IL-1β further exert negative feedback regulation on the TLR4/MyD88/NF-κB pathway, creating an inflammatory cascade that ultimately leads to the occurrence and progression of CRC (Zhu et al., 2019). Research indicates that the expression levels of TLR4 and NF-κB are significantly elevated in the colonic tissues of AOM/DSS-induced CAC mice as well as in human colorectal cancer tissues (Zhao et al., 2023; Xiaoping et al., 2023; Huang et al., 2014). Extensive evidence also suggested that MyD88-dependent NF-κB signaling pathway can be triggered by microbial infection or tissue damage, and the activation of NF-κB is enhanced in CRC. This finding suggested that the constitutive activation of NF-κB enhances inflammation in patients with colitis and contributes to colitis-induced carcinogenesis (Abdullah et al., 2013; Fukata et al., 2011; Hausmann et al., 2002; Peterson and Artis, 2014; Ullman and Itzkowitz, 2011). Inactivating the TLR4/NF-κB signaling pathway can alleviate oxidative stress and inflammatory responses in human colonic cells (Sun et al., 2020). Therefore, the TLR4/MyD88/NF-κB signaling pathway may represent a potential therapeutic target for CAC intervention. Inhibiting the expression of this signaling pathway could effectively suppress the occurrence and progression of colitis to CAC.

In recent years, the use of natural anti-cancer components found in food to intervene in tumor formation and prevent its further development has become an actively explored area in the field of nutrition. Tocotrienols is a subtype of vitamin E, naturally found in palm oil, rice bran, and annatto seeds. Its main structure consists of a chromanol ring with an isoprenoid side chain. Depending on the composition of the phytyl tail, tocotrienols can be divided into four isomers (α-, β-, γ-, or δ-) (Mohd Zaffarin et al., 2020). Studies shown that compared to other forms of vitamin E, γ-tocotrienol and δ-tocotrienol exhibit stronger anti-inflammatory and anti-tumor biological activities (Jiang et al., 2008; Yang et al., 2020). They selectively inhibit the proliferation of colon cancer cells, induce apoptosis in tumor cells (Husain et al., 2019; Xu et al., 2012), and suppress angiogenesis (De Silva et al., 2016; Li et al., 2011; Shibata et al., 2009). δ-tocotrienol has been found to inhibit inflammation through the MAPK and PPAR signaling pathways in LPS-stimulated macrophages (Shen et al., 2018). Similarly, γ-tocotrienol inhibits IL-6 production and NF-κB-activated in LPS-induced RAW264.7 macrophages (Wang and Jiang, 2013). Accumulating evidence suggests that tocotrienols possess effective anti-cancer properties by inhibiting the constitutive activity of NF-κB in various types of cancer, such as pancreatic and breast cancer (Popivanova et al., 2008; Di Martino et al., 2016). However, the inhibitory effects of tocotrienol on CAC and its regulation role on the TLR4/MyD88/NF-κB signaling pathway remain unclear.

Our previous research have found that both δ-tocotrienol and γ-tocotrienol effectively inhibited the proliferation of colon cancer cells SW620 (Zhang et al., 2011; Zhang et al., 2013). In a subsequent study, we observed that tocotrienol-rich fraction could suppress the growth of human colon cancer in xenografts nude mouse tumor model (Zhang et al., 2015). Enzyme-linked immunosorbent assays revealed that annatto tocotrienol could reduce the expression of NF-κB and MyD88 in colon cancer tissues (Qian et al., 2021).

In this study, we focused on the annatto tocotrienol, a natural compound abundant in delta-tocotrienol and gamma-tocotrienol. Our objective was to evaluate its therapeutic potential in a mouse model of colitis-associated cancer (CAC) and to elucidate its regulatory influence on the TLR4/MyD88/NF-κB signaling pathway. We aimed to establish annatto tocotrienol as a promising candidate for modulating the aberrant cytokine expression in CAC and for impeding tumorigenesis.

2. Materials and methods

2.1. Materials and reagents

Tocotrienol, which was extracted from annatto seeds, containing 89.2 % δ-tocotrienol and 10.8 % γ-tocotrienol, was provided by the American River Nutrition, Inc. (Hadley, MA, USA). Tocotrienol was premixed with soybean oil (Fulinmen First Grade Soybean Oil, 900 ml) before being provided to mice to avoid decreasing the biological activity of tocotrienol. Test compounds should be prepared once a week. AOM and DSS were purchased from Sigma-Aldrich (St Louis, MO, USA) and MP Biochemicals Inc. (Solon, OH, USA), respectively. PE-Cy™7 CD3e, PE CD4, and FITC CD8 and CBA Mouse Th1/Th2/Th17 Cytokine Kit were obtained from BD Biosciences (San Diego, CA, USA). Rabbit anti-NF-κB p65 and anti-MyD88 antibodies were obtained from Abcam. Mouse cytokine/chemokine magnetic bead panel was obtained from EMD Millipore (Billerica, MA, USA). TLR4, TRAF6 and β-actin antibodies were obtained from Bio-world (Minnesota, USA).

2.2. Animal treatment

Male CD-1 (ICR) mice (5 weeks old, 20–25 g) were obtained from Charles River (Beijing, China). These mice were housed in a specific pathogen-free condition and kept in the institute's animal facility for 1 week for adaptation. The bedding is SPF-grade corn cob bedding − eight mesh size. Mice were randomly divided into five groups (n = 20/group and 10 mice per cage), including Blank group, Model group, three different dosages δ-tocotrienol groups (Low dose group [50 mg/kg], Medium dose group [75 mg/kg], and High dose group [100 mg/kg]) (Qian et al., 2021). The CAC mouse model induced by AOM/DSS was established based on previous studies (Tanaka et al., 2003; Suzuki et al., 2005; Neufert et al., 2007). In generating a CAC model, mice were intraperitoneally injected with AOM at a concentration of 10 mg/kg body weight. Seven days after the AOM injection, the animals were

provided with 3 % DSS (w/v) in their drinking water for 1 week, followed by a 2-week period of regular water. This cycle of DSS treatment (1-week 3 % DSS+2-week water) was repeated for two additional cycles. In the 20-week observation period, CD-1 (ICR) mice in the tocotrienol groups were administered daily doses of 50, 75, and 100 mg/kg of δ-tocotrienol for three days prior to receiving an injection of AOM. The blank control group was consistently provided with normal drinking water and feed, and was not exposed to AOM, DSS, and tocotrienols. In our preliminary experiments, we observed no adverse effects on food and water intake in mice due to the tocotrienol supplementation (Qian et al., 2021). Daily assessments were performed on the mice to evaluate their general health, including the evaluation of coat quality, blood in stool, and diarrhea, as well as to ensure the continuous availability of food and water. Furthermore, weekly body weight measurements were taken to confirm adequate nutritional intake. Animals were euthanized using cervical dislocation method.

All animals were euthanized at the end of the study (week 20, Table 1). The blood was collected in heparinized-capped vials, and the plasma was separated by centrifuging blood at 4000 rpm for 15 min and then stored at −20℃. After the removal, blotting, drying, and weighing, the colon and spleen tissues were isolated, and part of the tissues were fixed in 10 % formalin. The remaining tissues were immediately stored at −80℃.

The experimental protocol was approved by the Committee on the Ethics of animal experiments of the Tianjin Center for Disease Control and Prevention. This study was carried out in strict accordance with The People's Republic of China Laboratory Animal Regulations.

2.3. Histological of colon and spleen

Resected mice colon and spleen tissues were fixed in neutral 10 % formalin for 48 h at room temperature, dehydrated in ethanol, cleared in xylene, and embedded in paraffin. Sections with a thickness of 4 μm were stained with hematoxylin and eosin (H&E) and analyzed for tumor evaluation and inflammation by pathologists. Resected mice colon and spleen tissues were fixed in neutral 10 % formalin for paraffin embedding. Paraffin-embedded sections were cut into 4 μm, deparaffinized, rehydrated, and pretreated with 1 % H_2O_2 solution for the immunohistochemical detection of cells positively stained with antibodies against MyD88 and NF-κB. Quantification was performed using the Image-Pro Plus 6.0 Software (Media Cybernetics, Bethesda, MD, USA) for analyzing the protein expression.

2.4. Flow cytometric (FACS) analysis

The peripheral blood was clotted for 2 h at room temperature and then centrifuged for 15 min at 1000 × g. The serum was removed, and the samples were stored at −80 ℃. The serum was incubated with the mixed capture beads at room temperature for 2 h, which were protected from light. Wash buffer was added to the tube and centrifuged at 200 g for 5 min. The supernatant was carefully aspirated and then discarded from the tube. Wash buffer was added to the tube to resuspend the bead pellet. The results were analyzed using FACS Canto II (BD Bioscience, Franklin Lakes, NJ, USA) and FACP Array v3.0.

Table 1
Effects of annatto-tocotrienol on hematochezia and tumor formation in mice.

Groups	Hematochezia (%)			Tumor formation (%)
	6th week	9th week	20th week	
Blank group	0 (0/20) *	0 (0/20) *	0 (0/20) *	0 (0/20) *
Model group	55 (11/20)	68.42 (13/19)	100 (15/15)	100 (15/15)
Low dose group	50 (9/18)	61.11 (11/18) *	75.00 (12/16)	75.00 (12/16)
Medium dose group	40 (8/20)	55.00 (11/20) *	76.47 (13/17)	70.59 (12/17)
High dose group	40 (8/20)	50.00 (10/20) *	72.22 (13/18)	44.44 (8/18) *
χ^2	16.03	23.28	45.11	41.72
P	0.003	< 0.001	< 0.001	< 0.001

*$P<0.05$ compared with the Model group.

2.5. Mouse Luminex assay

The blood was allowed to clot for at least 30 min before centrifugation for 10 min at 1000 × g. The serum was removed, and assay was performed immediately or aliquot and the samples were stored at ≤ −20℃. Serum samples should be diluted at 1:2 in the assay buffer provided in the kit. The serum IL-4 and Macrophage Inflammatory Protein (MIP) −1β concentrations were analyzed by Luminex assay according to the manufacturer's suggested instructions.

2.6. Immunohistochemical analysis

After placing the colon in a 10 % formalin fixation solution for 48 h, the tissue was sequentially dehydrated, cleared, and wax-impregnated. It was then embedded in an automatic biological tissue embedding machine with section thicknesses of 4 μm. The tissue sections were placed on glass slides and dried at 60℃. The sections were immersed in xylene for 5 min each time, for a total of two immersions to achieve dewaxing. Subsequently, the sections were sequentially immersed in 100 % ethanol for 1 min (twice), 95 % ethanol for 1 min (twice), and 80 % ethanol for 1 min (twice), followed by rinsing with distilled water 1–2 times and 0.1 M PBS twice. The sections were incubated in 1 % methanol hydrogen peroxide at room temperature for 10 min, rinsed once with distilled water, and washed with 0.1 M PBS three times, 5 min each. The sections were placed in 0.01 M citrate buffer (pH 6.0) and boiled for 15–20 min, then cooled to room temperature, and washed with 0.1 M PBS three times, 5 min each. Goat serum blocking solution was added to the sections and incubated at room temperature for 20 min, then the excess liquid was discarded. Primary antibodies (Rabbit anti-NF-κB p65, anti-MyD88 antibodies, Abcam) were added to the sections and incubated overnight at 4℃, followed by washing with 0.1 M PBS three times, 5 min each. Biotinylated secondary antibody (Bioworld, Minnesota, USA) was added to the sections and incubated at 37℃ for 20 min, then washed with 0.1 M PBS three times, 5 min each. The sections were treated with S-A/HRP and incubated at 37℃ for 20 min, then washed with 0.1 M PBS three times, 5 min each. DAB chromogenic reaction was performed, followed by thorough washing to stop the reaction. The cell nuclei were counterstained with hematoxylin for 2 min, then thoroughly washed, differentiated with 0.5 % hydrochloric acid alcohol for 5 s, and rinsed with running tap water for 15 s. After dehydration and clearing, the sections were mounted with neutral balsam. The tissue sections were observed and recorded under a microscope and analyzed using Image-ProPlus software.

2.7. Western blot analysis

Retrieve a sample of distal colon tissue and carefully place it into a pre-chilled glass homogenizer. Ensure to homogenize the tissue thoroughly. Transfer the homogenized liquid to a new EP tube and extract proteins by lysing in an ice-water bath. Using the BCA protein assay to assess for protein content. Protein samples were combined with SDS-PAGE sample loading buffer and subjected to boiling for denaturation for a duration of 10 min. Following cooling to room temperature, the protein samples were then loaded into the wells of the SDS-PAGE gel for electrophoretic separation and subsequent transfer onto a PVDF membrane. The membrane was then immersed in a Western blotting blocking solution and incubated on a slow shaker at 37℃ for a minimum of 1 h. The samples were then incubated overnight at 4℃ with antibodies specific to MyD88 (Abcam), NF-κB (Abcam), TRAF6 (Bioworld), TLR4

(Bioworld), and β-actin (Bioworld). After being washed with TBS-T solution, the secondary antibody (Bioworld) was added, and the samples were incubated on a shaker at room temperature for two hours. Chemiluminescence was employed for color development. The PVDF membrane, which had been incubated with the secondary antibody and washed, was placed in a gel imaging system (Shanghai Tianneng Technology Co., Ltd., Model: VE-180). The gel imaging system software was initiated, the chemiluminescence option was selected, and the membrane was exposed and photographed.

2.8. Statistical analyses

Statistical analyses were performed using SPSS statistics 20.0. Qualitative data are presented as rates and composition ratios. To assess differences between groups, the chi-square test is employed, and for pairwise comparisons within groups. For quantitative data that are normally distributed, the mean ($\overline{X}$) ± standard (SD) deviation is used for representation. Group comparisons are conducted using one-way ANOVA, and for post-hoc pairwise comparisons, the Bonferroni correction method is applied. Differences in survival between groups were compared using the log-rank test, and the differences in body weight among groups were compared using repeated-measures ANOVA. $P<0.05$ was considered statically significant. All statistical tests were two-sided.

3. Results

3.1. Effects of tocotrienol treatment on colitis and CAC development in mice

To assess whether tocotrienol regulates immune function in CAC, we treated CD-1 (ICR) mice with AOM and DSS. As shown in Fig. 1A, the body weight showed an increasing state in each group, but the differences among groups were significantly different among all groups ($P>0.05$). No deaths or hematochezia were observed in the control group throughout the course of the experiment (Fig. 1B and Table 1). Compared with the blank group, the survival rate of model group (25.0 %) was significantly decreased. Following the experiment, the survival rates of the model group, low-dose group, medium-dose group, and high-dose group were 51.1 %, 62.9 %, and 60.0 %, respectively (Fig. 1B).

Since the 6th week, colonic cancer model groups showed visible blood in the stool. The incidence of blood stool in colonic cancer model groups was statically significantly increased compared with that in the blank group at the 6th, 9th, and 20th week. The incidence of blood stool was 68.42 % (13/19) in the model group at the 9th week, and the incidence reduced to 61.11 % (11/18), 55 % (11/20), and 50 % (10/20) following tocotrienol treatments of 50, 75, and 100 mg/kg· bw, respectively (Table 1). The gross examination of colon tissues indicated that while typically solid tumors were observed in mice in the model group, low dose group, medium dose group, and high dose group after 20 weeks, the tumor incidences were 100 % (15/15), 75 % (12/16), 70.59 % (12/17) and 44.44 % (8/18), respectively (Table 1). Compared

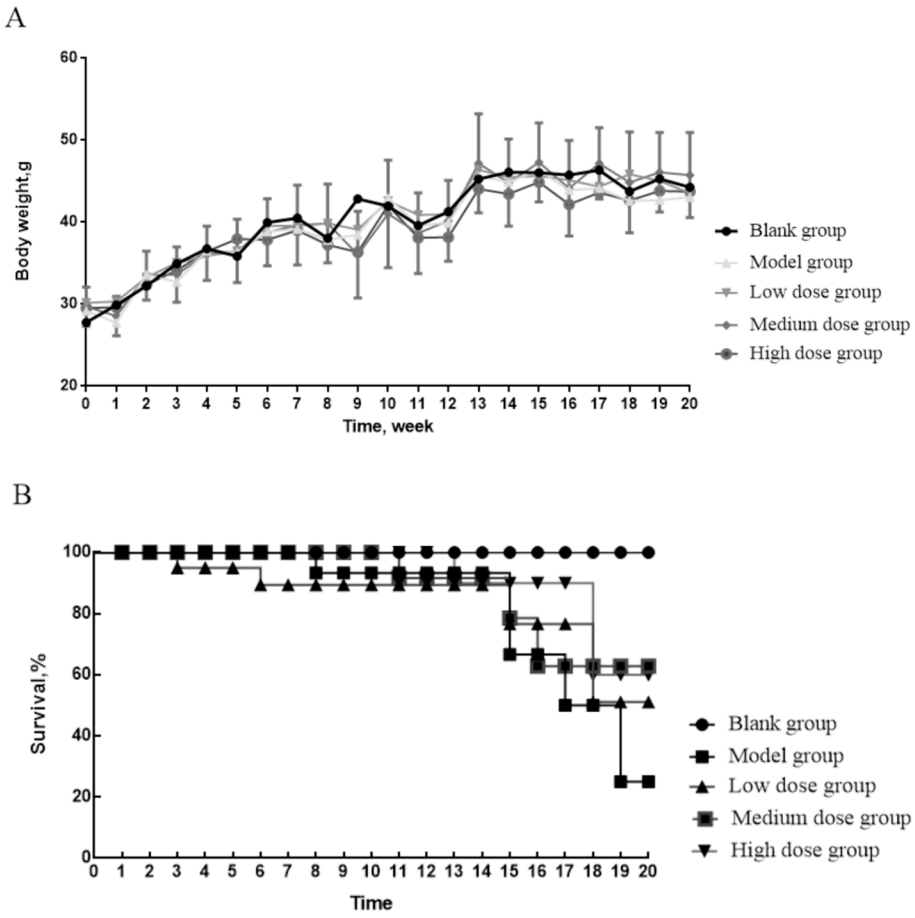

Fig. 1. Effects of annatto-tocotrienol on the body weight and survival in mice. A. Changes of body weight in the mice model for 20 weeks, Repeated measures ANOVA. The number of mice is as follows: Blank group, n = 20; Model group, n = 15; Low dose group, n = 16; Medium dose group, n = 17; High dose group, n = 18. B Survival curves in mice, Survival analysis. The data are presented as the mean ± SD. *$P<0.05$ compared with the model group.

with the model group, the tumor incidence in the high dose group was significantly reduced ($P<0.05$) (Table 1).

AOM/DSS can also significantly increase the organ coefficients of colon and spleen, and annatto-tocotrienol treatment decreased these organ coefficients (Fig. 2). The H&E staining of colon tissues and spleen was performed to analyze the pathology of AOM/DSS- induced colons. As shown in Figs. 3 and 4, Model group had adenoma in the distal colon, and the size and shape of cells were different. The number of splenic nodules was reduced, and the red marrow cells were sparse. Tocotrienol treatment inhibited the development of CAC and ameliorated the phenomenon of spleen lesion in mice induced by AOM/DSS treatment. The number of spleen nodules in the medium dose group increased slightly, the margin area was widened, and the degree of inflammation of the colon was minimal. The results demonstrate that tocotrienol can inhibit colorectal tumorigenesis induced by AOM/DSS.

3.2. Effects of tocotrienol treatments on IL-6, TNF-α, and IL-10 production in mice with CAC

To explore the influences of different tocotrienol treatments on inflammation cytokine production in CAC mice, we measured the TNF-α, IL-6, and IL-10 levels by flow cytometric analysis. Following AOM/DSS treatment, the IL-6 and TNF-α concentrations increased, whereas IL-10 levels reduced (Fig. 5). Compared with the model group, the IL-6 concentration significantly decreased in the blank group, low dose group, medium dose group and high dose group ($P<0.05$, Fig. 5A). Compared with the model group, the TNF-α concentration significantly decreased in the blank group, low dose group, medium dose group and high dose group reduced ($P<0.05$, Fig. 5B). IL-10 levels were increased in blank group, medium dose group and high dose group, compared with model group ($P<0.05$, Fig. 5C). The current studies demonstrate that tocotrienol significantly attenuates the serum IL-6 and TNF-α levels that are elevated in response to AOM/DSS treatment.

3.3. Effects of tocotrienol treatment on IL-4 and MIP-1β levels in mice with CAC

We investigated the levels of IL-4 and MIP-1β in mice treated with AOM/DSS. Results showed an increase in MIP-1β levels in the model group, whereas the IL-4 level decreased (Fig. 6). Compared with the model group, the IL-4 concentration increased in the low dose group, medium dose group and high dose group, but the differences were not statistically significant ($P>0.05$, Fig. 6A). Compared with the model group, the medium dose and high dose tocotrienol treatments reduced the MIP-1β concentration in the serum (Fig. 6B).

3.4. Effects of tocotrienol treatments on MyD88 and NF-κB expression in mice

To address the role of TLRs in tumorigenesis and progression in CAC, we examined MyD88 and NF-κB protein expression levels by IHC. IHC analysis demonstrated that the expression of protein MyD88 was significantly elevated in the model group and low dose group compared with that in the blank group. Meanwhile, the expression was reduced by tocotrienol treatment (Figs. 7 and 9A). IHC analysis demonstrated that the protein NF-κB expression was significantly increased in the model group and low dose group compared with the blank group. Meanwhile, the expression was significantly reduced by tocotrienol treatment (Figs. 8 and 9B).

3.5. Tocotrienol down-regulated TLR4/MyD88/NF-κB signaling pathway

We found that tocotrienol inhibited the expression of activated TLR4/Myd88/NF-κB signaling pathway proteins such as TLR4, MyD88, TRAF6 and NF-kB. Compared with blank group, expressions of TLR4, MyD88, TRAF6 and NF-κB increased in model group ($P<0.05$, Fig. 10). The results showed that tocotrienol had different effects on these protein expressions in mice with CAC. Compared with model group, expressions of TLR4 and MyD88 were decreased in medium dose group and high dose group ($P<0.05$). Compared with model group, expressions of NF-κB were decreased in low dose group, medium dose group and high dose group ($P<0.05$). Compared with model group, the expression of TRAF6 was decreased in high dose group ($P<0.05$).

Discussion

CAC is a malignancy of the colon that results from IBD (Terzić et al., 2010). Previous studies on CAC have revealed that blocking the inflammatory pathway is not only significantly associated with the protection against DSS-induced colonic tumors but is also effective in preventing CAC in both preclinical and clinical studies (Popivanova et al., 2008; Di Martino et al., 2016; Rostom et al., 2007). Nonsteroidal anti-inflammatory drugs, as potential chemo-preventive agents for colorectal cancer, can reduce the risk of developing colonic tumors (Garcia Rodriguez et al., 2013). Nevertheless, long-term use can lead to various side effects, including nausea, dyspepsia, and gastrointestinal bleeding (Serebruany et al., 2004). Therefore, the discovery and utilization of novel drugs with minimal adverse effects are imperative. In the

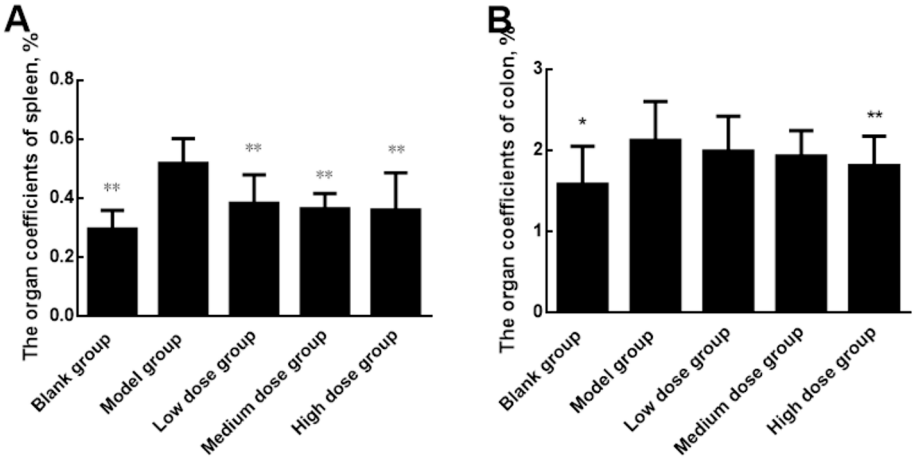

Fig. 2. Effects of annatto-tocotrienol on the organ coefficients in mice. (A) The organ coefficients of spleen in each group. (B) The organ coefficients of colon in each group. The data are presented as mean ± SD. Group comparisons were analyzed using ANOVA. Pairwise comparisons were conducted using the Bonferroni method. *$P<0.05$ compared with the model group; **$P<0.01$ compared with the model group.

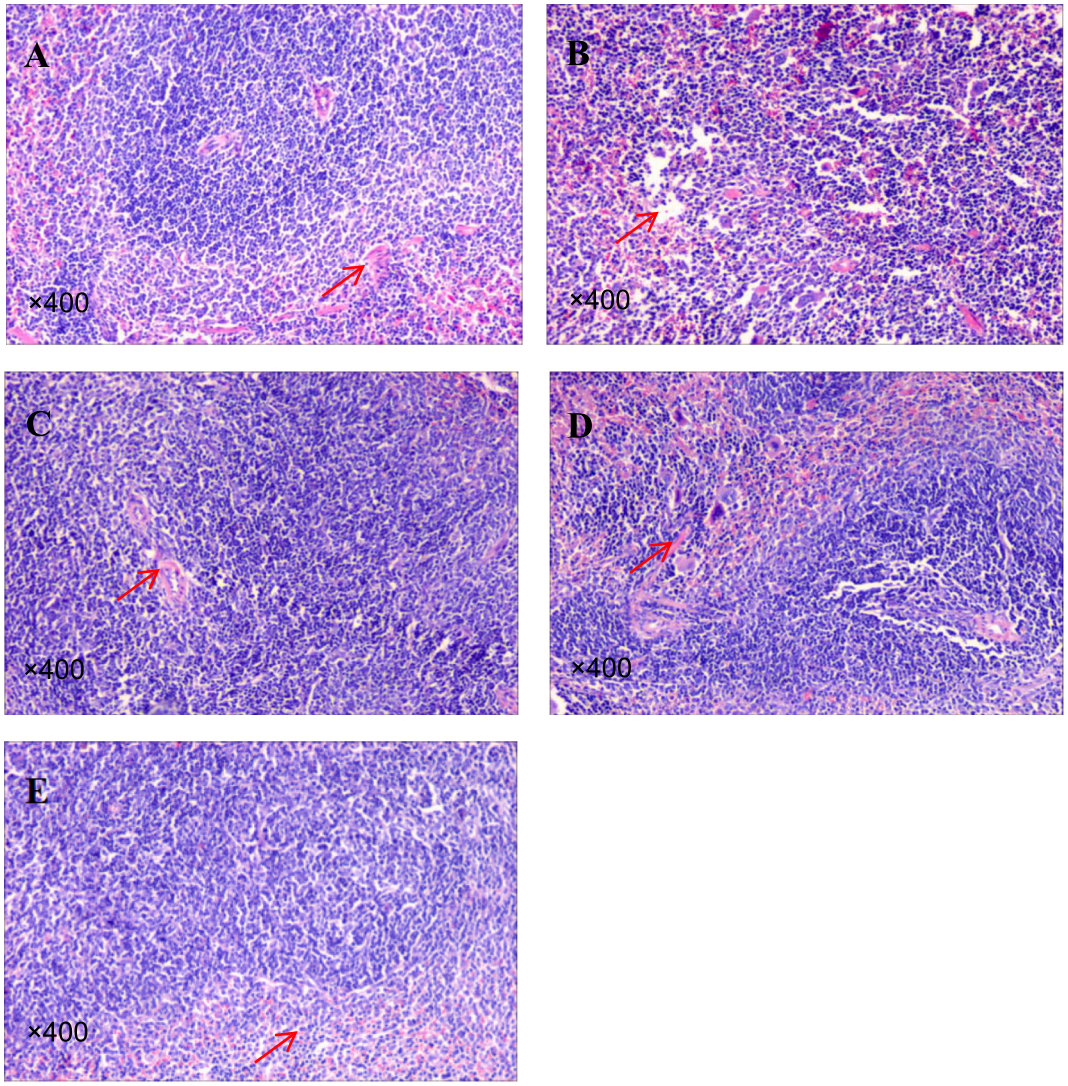

Fig. 3. Pathological changes of spleen in mice. A) Blank group (400 ×). B) Model group (400 ×). C) Low dose group (400 ×). D) Medium dose group (400 ×). E) High dose group (400 ×). The blank group had a smooth tunica serosa. The red and white pulp structures of the spleen were clear, with the red pulp spleenic sinuses filled with red blood cells, and there was no increase or decrease in the number of splenic nodules in the white pulp. In the model group: the number of splenic nodules decreased, the structure of the nodules and the marginal zone were less clear, and the lymphocytes in the red pulp were sparse. In the low dose group, medium dose group and high dose group, the number of splenic nodules, the structure of the splenic nodules, the structure of the marginal zone, and the content of lymphocytes in the red pulp tended to improve or recover close to the control group. (For interpretation of the references to color in this figure legend, the reader is referred to the web version of this article.)

present study, we selected annatto-tocotrienol, a natural compound in annatto beans which can significantly inhibit colon cancer initiation and suppress colitis-associated tumorigenesis, and we further described its underlying mechanisms.

In this study, AOM/DSS induced mouse model of CAC cancer was established. This model was used to evaluate the preventive and therapeutic effects of tocotrienol in CRC mice and its regulatory effect on TLR4/MyD88/NF-κB pathways. Our results showed that with the increase in modeling time, CD-1 (ICR) mice in the colon cancer model group all exhibited visible hematochezia (Table 1), and the mortality rate of the mice gradually increased (Fig. 1). This finding is consistent with the results of Suzuki et al (Suzuki et al., 2004). At the end of the experiment, multiple colon tumors were observed in the mice. Histological analysis of the colon in the model group revealed varying degrees of epithelial cell shedding, loss, glandular destruction, adenomatous structures, phosphorylation of epithelial cells in some mice, and infiltration of inflammatory cells primarily composed of lymphocytes, consistent with the typical pathological changes of inflammation-related colon cancer (Fig. 4B). The number of animals in the tocotrienol groups exhibiting visible rectal bleeding and mortality was lower than that in the model group (Fig. 1). Pathological analysis revealed a reduction in the inflammatory response in tocotrienol groups (Fig. 4C-E). Therefore, this experiment successfully induced CRC in mice. Although tocotrienol increased the survival rate of CRC mice, reduced the number of mice with rectal bleeding and tumor formation, inhibited colon weight gain in mice with colon cancer, and alleviated the infiltration of inflammatory cells in the colon tissue of AOM/DSS-induced mice. However, the damage to the colon tissue was still quite severe, which may be related to the long duration of modeling or insufficient dosage of tocotrienol.

Studies have shown that the inflammatory microenvironment surrounding intestinal epithelial cells in patients with inflammatory bowel disease plays an important role in carcinogenesis and inflammation-related epithelial cell damage and repair, which promotes CAC development (Saleh and Trinchieri, 2011; Xie et al., 2016). Microbial infection or tissue injury induces inflammatory responses by activating the TLR/MyD88 signaling pathway (Akira et al., 2001).

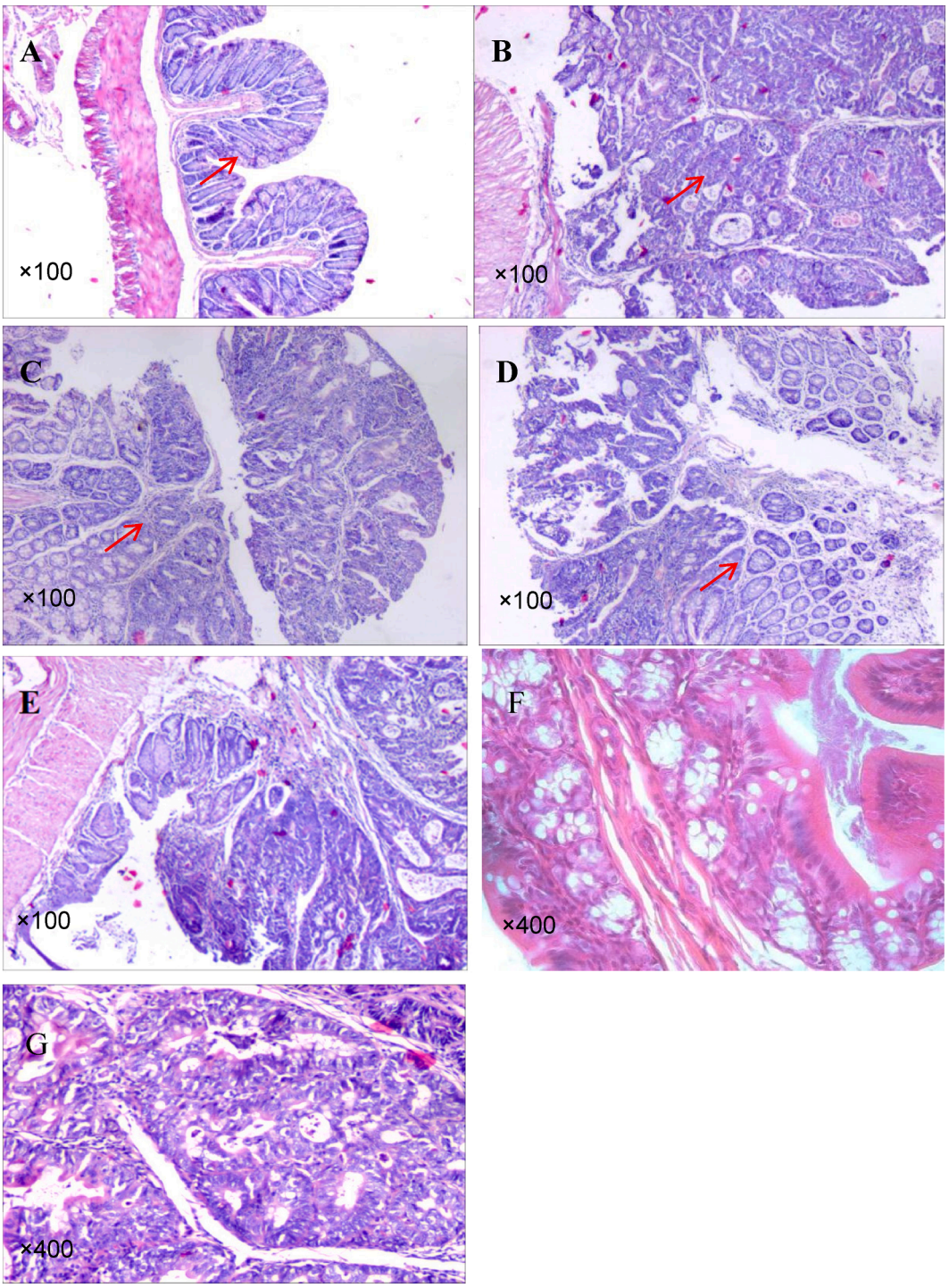

Fig. 4. Pathological changes of colon in mice. A) Blank group (100 ×). B) Model group (100 ×). C) Low dose group (100 ×). D) Medium dose group (100 ×). E) High dose group (100 ×). E) Blank group (400 ×). F) Model group (400 ×). Under the microscope, the blank group showed that the intestinal glandular epithelial cells were arranged in a single layer of columnar cells with normal size and morphology. In the model group, the mice displayed adenomatous structures with pseudostratification, loss of cell polarity, inconsistent cell size and morphology, deepened nuclear staining, and other obvious atypical features, involving cases from the mucosal layer to the submucosal layer. The tumor formation rate in the model group was 100 %, in the tocotrienol high-dose group was 84 %; in the tocotrienol medium-dose group was 88 %; and in the tocotrienol low-dose group was 84 %.

TLR4 signaling consist of MyD88-dependent and Myd88-independent pathways (Dunne and O'Neill, 2003; Leulier and Lemaitre, 2008). TLR4 expression in colitis mice induced by DSS and TNBS is significantly increased with the upregulation of NF-κB expression, suggesting that the MyD88/NF-κB pathway plays an important role in IBD. Similar phenomena were observed in the human intestinal epithelial cells of patients with inflammatory bowel disease. This study obtained similar results. The expression of key factors in the TLR4/MyD88/NF-κB pathway was examined. Compared to the blank group, the expression levels of TLR4, MyD88, TRAF-6, and NF-κB p65 in the colon tissue of the AOM/DSS model mice were significantly increased, and after treatment with tocotrienol, their expression levels significantly decreased (Figs. 7-10). Immunohistochemistry showed that MyD88 was primarily located in the cytoplasm (Fig. 7), while NF-κB was mainly located in the nucleus

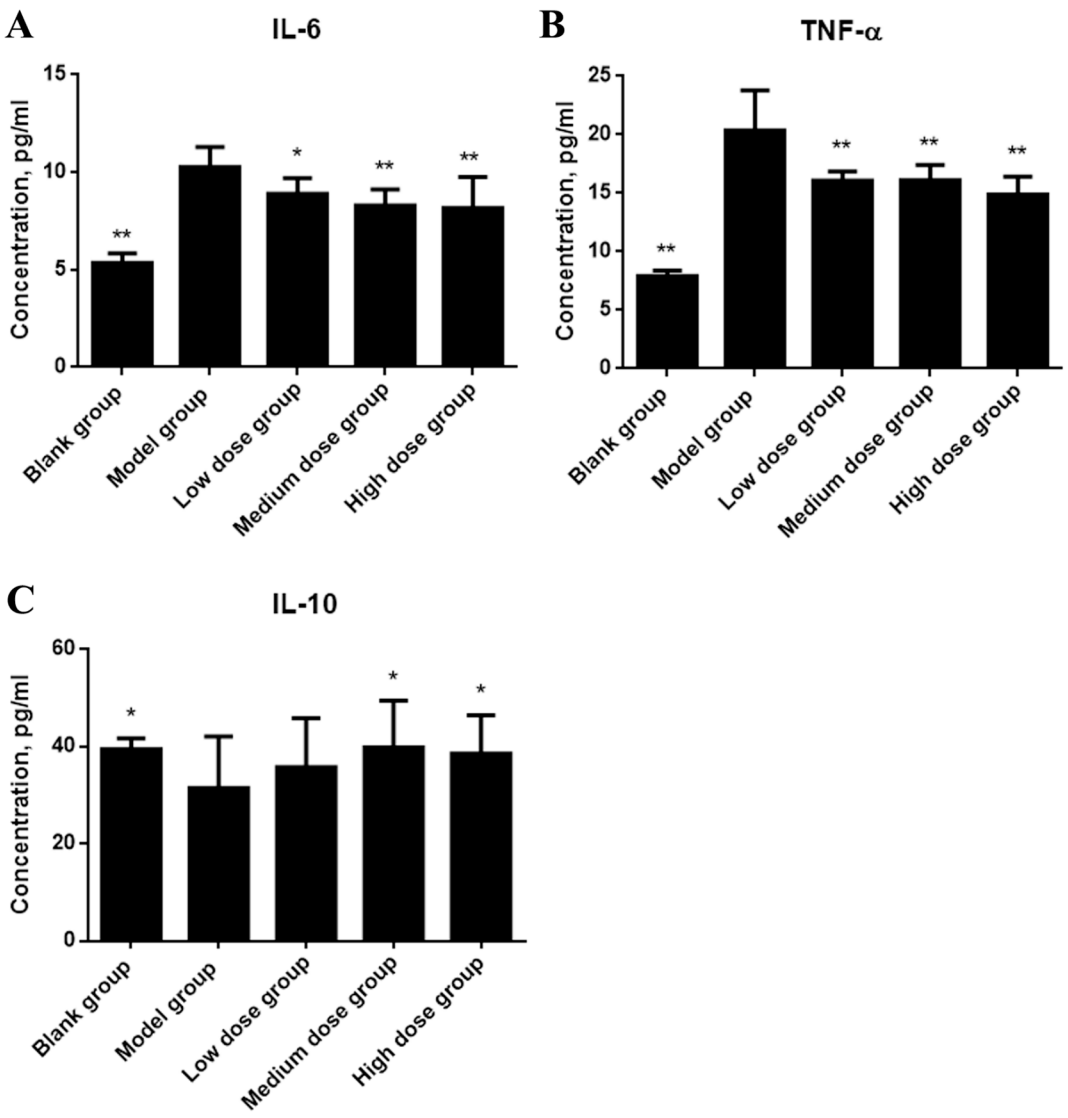

Fig. 5. Effects of annatto-tocotrienol on the IL-6, TNF-α, and IL-10 levels in mice. The IL-6 (A), TNF-α (B), and IL-10 levels in the serum were measured in mice by flow cytometry (FACS). Group comparisons were analyzed using ANOVA. Pairwise comparisons were conducted using the Bonferroni method. The data are presented as mean ± SD. $^{*}P<0.05$ compared with the blank group; $^{**}P<0.01$ compared with the blank group.

(Fig. 8).

The abnormal activation of NF-κB can lead to the occurrence and development of tumors, such as colon cancer, breast cancer, and prostate cancer. The TLR signaling pathway promotes NF-κB activation by TLRs and other microbe-sensitive factors. The activated NF-κB can elevate the expression of inflammatory cytokines and induce inflammatory responses; subsequently, it contributes to tumorigenesis and induces tumor cells to secrete inflammatory cytokines, evades the host immune system, and avoids the attack by CTL and NK cells, thereby promotes the growth and migration of tumor cells (Szajnik et al., 2009; He et al., 2007). Xie et al (Xie et al., 2016) found that the MyD88 inhibitor (TJ-M2010-5) treatment significantly inhibits AOM/DSS-induced colitis, completely prevents CAC development, suppresses cell proliferation, increases apoptosis in colon tissue, and reduces the production of inflammatory cytokines and chemokines, as well as the infiltration of immune cells in colon tissue. Therefore, the activation of TLR/MyD88/NF-κB signaling pathway may be a new potential target for tumor development. The intervention of the MyD88-dependent signaling pathway to improve the inflammatory response of the immune system plays an important role in the development of tumor. Our data shows that annatto-tocotrienol inhibits the activation of MyD88 and NF-κB and then inhibits CAC development, improves CAC mice survival, and provides preclinical evidence of its anticancer effect.

Numerous studies have confirmed that lymphocytes and cytokines play a crucial role in the pathogenesis of CAC. In this study, we observed that the peripheral blood levels of TNF-α in the model group mice were higher than those in the blank group and the tocotrienol intervention group (Fig. 5B). TNF-α, secreted by tumors and tumor-associated macrophages, is one of the major inducible mediators involved in inflammation, apoptosis, and immune responses (Fonseca-Camarillo et al., 2018; Indaram et al., 2000). Boryana et al. demonstrated that TNF-α and its receptor TNF-Rp55 are overexpressed in the colon of wild-type mice treated with AOM and DSS, while no elevation was observed in transgenic mice lacking TNF-Rp55. TNF-α also plays a critical role in the pathogenesis of IBD, and TNF receptor (TNFR) expression is upregulated in the colonic epithelial cells in patients with ulcerative colitis and Crohn's disease (Tanaka et al., 2003; Popivanova et al., 2008). Thus, TNF-α is a crucial mediator in colon cancer initiation and progression.

IL-6 is a cytokine produced by mononuclear macrophages and activated T lymphocytes; Under normal physiological conditions, serum IL-6 levels are typically low. However, in patients with malignant tumors, serum IL-6 levels are significantly elevated compared to those in the

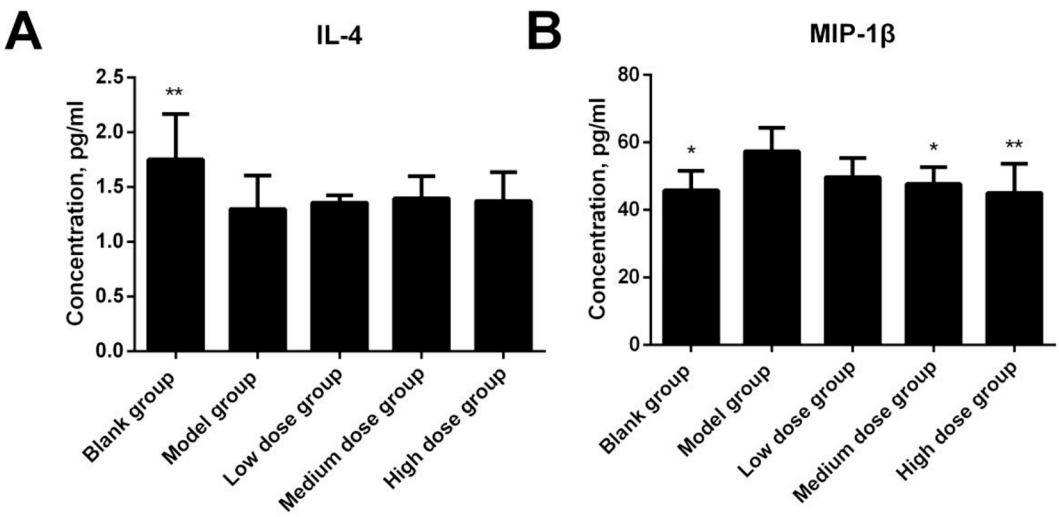

Fig. 6. Effects of annatto-tocotrienol on the IL-4 and MIP-1β levels in mice. The IL-4 (A) and MIP-1β (B) levels in the serum were measured in mice by Luminex assay. The data are presented as mean ± SD. Group comparisons were analyzed using ANOVA. Pairwise comparisons were conducted using the Bonferroni method. $^{*}P<0.05$ compared with the blank group; $^{**}P<0.01$ compared with the blank group.

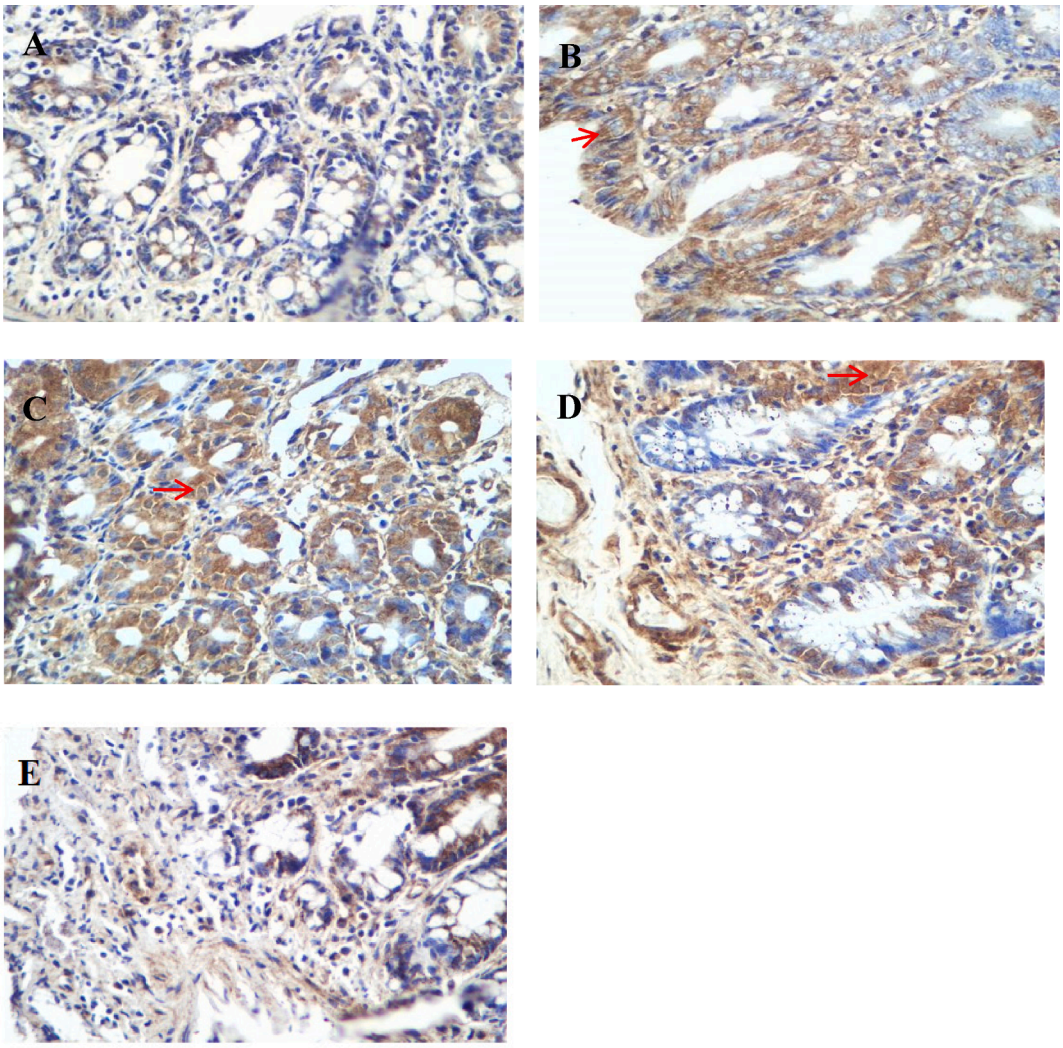

Fig. 7. MyD88 expression in the colon of mice treated with AOM/DSS or annatto-tocotrienol. MyD88 expression in mice colon in each group was determined by immunohistochemistry. Immunohistochemistry showed that MyD88 staining was mainly in the cytoplasm. A–E MyD88 expression in the blank (A, 400 ×), model (B, 400 ×), low dose group (C, 400 ×), medium dose group (D, 400 ×) and high dose group (E, 400 ×), respectively.

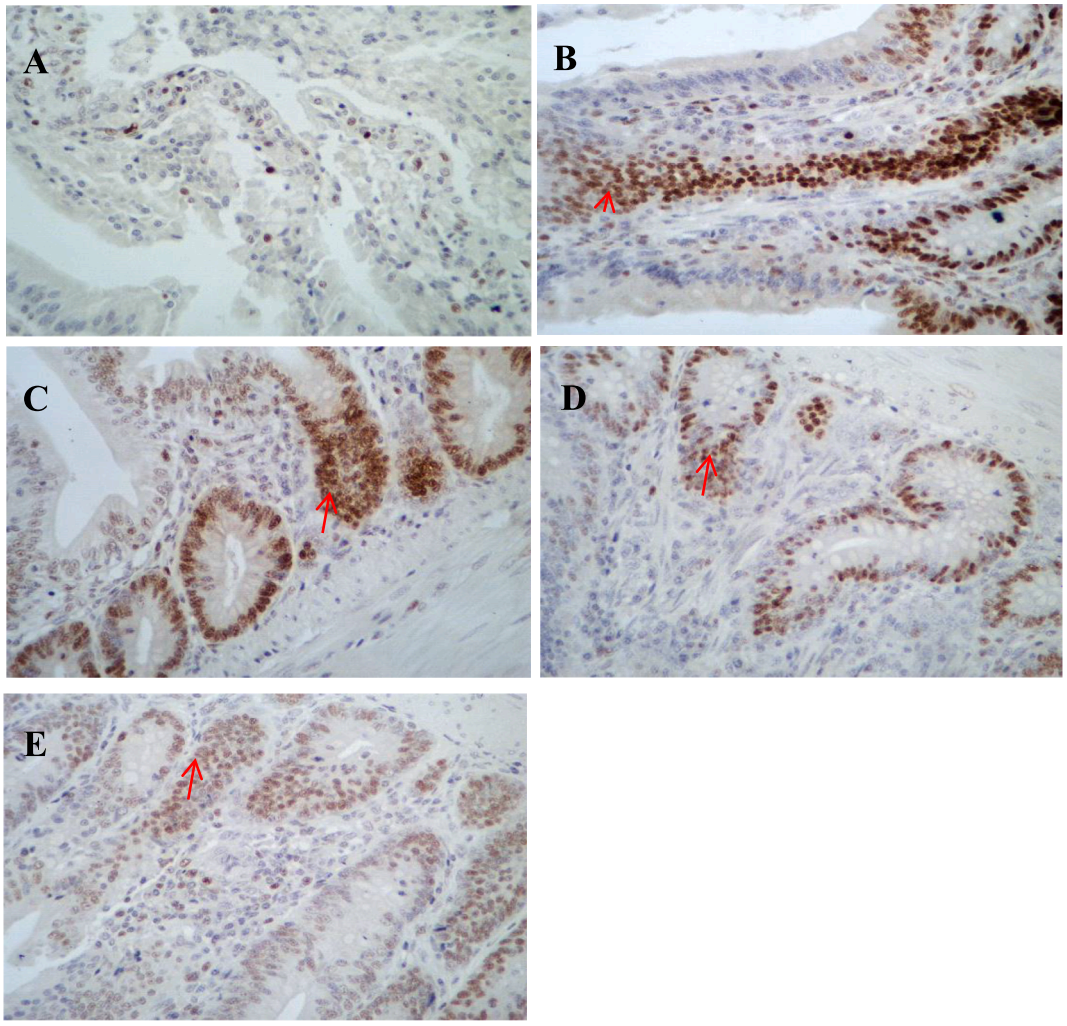

Fig. 8. NF-κB expression in the colon of mice treated with AOM/DSS or annatto-tocotrienol. NF-κB expression in mice colon in each group was determined by immunohistochemistry. Immunohistochemistry showed that NF-κB staining was mainly in the nucleus. A–E NF-κB expression in the blank (A, 400 ×), model (B, 400 ×), low dose group (C, 400 ×), medium dose group (D, 400 ×) and high dose group (E, 400 ×), respectively.

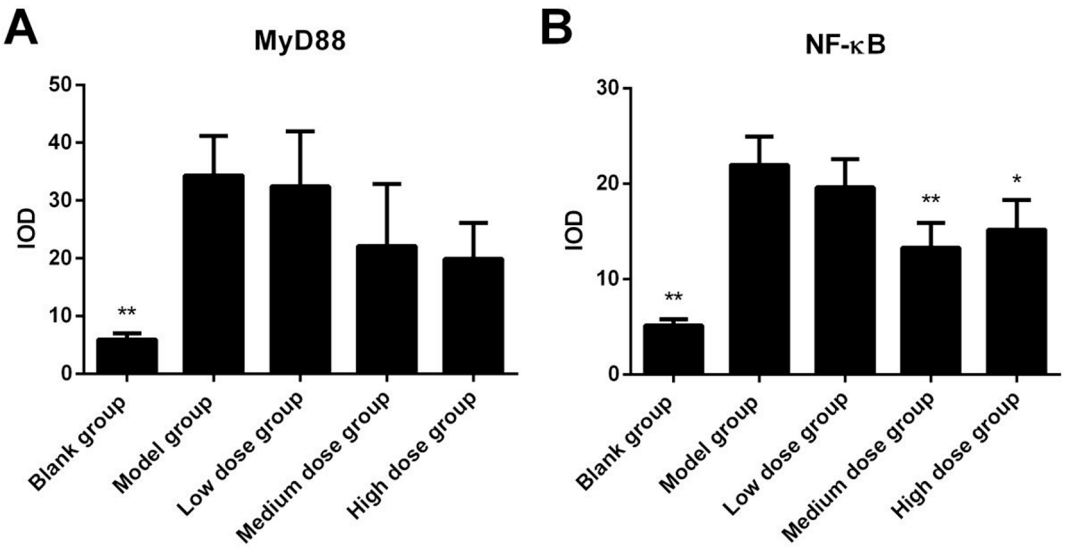

Fig. 9. MyD88 and NF-κB levels in the mice colon in mice. The total protein was extracted from mouse colon each group. The MyD88 and NF-κB levels were measured by IHC. The data are presented as mean ± SD. Group comparisons were analyzed using ANOVA. Pairwise comparisons were conducted using the Bonferroni method. $^{*}P<0.05$ compared with the Model group; $^{**}P<0.01$ compared with the Model group.

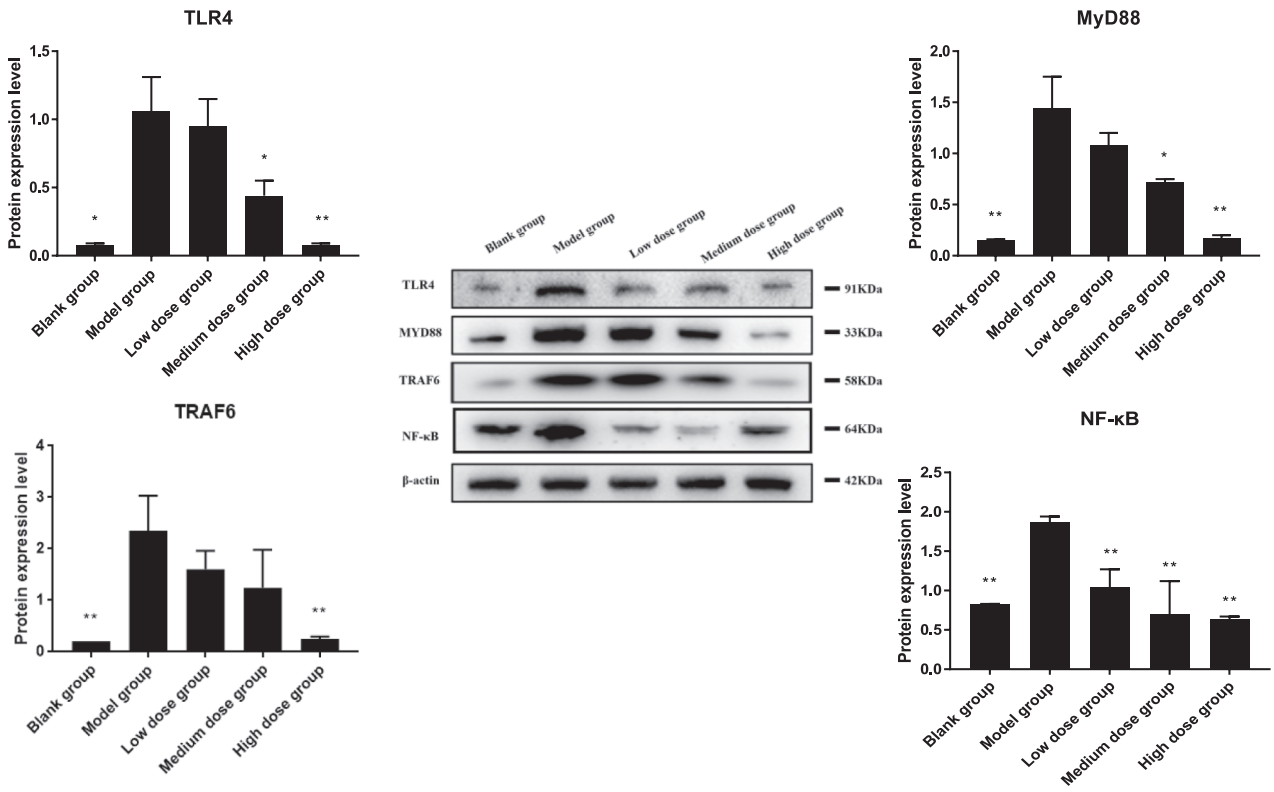

Fig. 10. The protein expression of TLR4, MyD88, TRAF6, NF-κB and β-actin in the mice colon in mice. The total protein was extracted from mice colon each group. The tissue were examined by western blotting as described in the Materials and Methods section. The data are presented as mean ± SD. Representative images of at least three independent experiments are shown. Group comparisons were analyzed using ANOVA. Pairwise comparisons were conducted using the Bonferroni method. *$P<0.05$ compared with the model group; **$P<0.01$ compared with the model group.

control group or patients with non-malignant conditions. Consequently, IL-6 has been proposed as a potential biomarker for the diagnosis of both inflammatory conditions and malignancies (Okayasu et al., 1996; Santiago, 2019; Yang, 2015). Serum and urine IL-6 levels are significantly elevated in patients following surgery, burns, spinal cord injuries, and infections (Codeluppi et al., 2014). The serum IL-6 level in patients with colon cancer was significantly higher compared to healthy individuals, and the IL-6 level in patients with advanced colorectal cancer was higher than that at an early stage. These results indicate that the expression of IL-6 in cancer patients is closely related to tumor size and metastasis; Higher plasma IL-6 levels are associated with the prognosis and pathogenesis of various cancers (Angevin et al., 2014; Munkholm, 2003; Murthy et al., 2023; Nagasaki et al., 2014; Scotti et al., 2024). In our study, the flow cytometry results showed that the peripheral blood levels of IL-6 in AOM/DSS-induced mice were higher than those in the control group, while the tocotrienol groups effectively reduced the expression of IL-6 (Fig. 5A). This finding is also consistent with the previous studies.

IL-4 is primarily secreted by Th2 cells, mediating inflammatory reaction caused by eosinophils, clearing extracellular pathogens, and participates in allergic reaction, and blocking the expression of IL-1β and TNF-α (Brown and Hural, 2017; Harvanová et al., 2023; Katz et al., 2001). The number of IL-4 secreting cells and the expression of IL-4 decrease in ulcerative colitis patients (ten Hove et al., 2004). Mittal et al (Mittal et al., 2005) found that the IL-4 levels in the ulcerate colitis group were significantly lower than that in the control group, the severity of colitis correlates negatively with IL-4 expression levels. After drug treatment, no significant difference in IL-4 levels was observed between the intervention group and the control, potentially due to the immune system's instability during the remission phase. Similar results were observed in this experiment, with IL-4 levels in the model group lower than in the blank group, and minimal changes noted in the annatto-tocotrienol groups (Fig. 6A).

IL-10 is mainly produced by monocytes, macrophages, and Th2 cells, acting as a negative regulator, blocking the secretion of chemokines, TNF-α, IL-6, and other cytokines, inhibiting the inflammatory responses, and regulating the proliferation and differentiation of various immune cells (Nagata and Nishiyama, 2021; Ribbons et al., 1997; Rutz and Ouyang, 2016). IL-10 (−/-) mice spontaneously develop intestinal inflammation characterized by discontinuous transmural lesions, thereby affecting both the small and large intestines and the dysregulated production of proinflammatory cytokines (Hurtubise et al., 2019). This study demonstrated that treatment with tocotrienol (50, 100 mg/kg BW) significantly increased the serum IL-10 level in AOM/DSS-induced CRC model group mice (Fig. 5C).

In the present study, a single injection of AOM followed by three cycles of DSS resulted in a 100 % incidence of CAC. Annatto-tocotrienol treatment inhibited the tumor growth and mortality induced by AOM/DSS, which was accompanied by a reduction of the number of tumor and colon shortening. In particular, tocotrienol can prevent the increase in spleen and colon organ coefficients (Fig. 2). The histological sections stained with H&E revealed that the colonic epithelium of control group mice was intact, with well-defined crypt depth, no infiltration of inflammatory cells in the mucosa and submucosa, and no ulceration or hyperemic edema. In contrast, the massive infiltration of lymphocytes was observed in the mucosa and submucosa in the AOM/DSS-induced mice, accompanied by dysplastic gland with hyperchromatic nuclei or adenomatous hyperplasia in colon epithelium. Additionally, the pleomorphism of tumor cells was improved in annatto-tocotrienol treatment groups. Our data shown that compared with the AOM/DSS group, the expression levels of MyD88 and NF-κB decreased in the annatto-tocotrienol groups. Annatto-tocotrienol inhibited CAC development by suppressing the activation of TLRs/MyD88 signaling pathway and improving the survival of CAC mice. We investigated the roles of lymphocyte and cytokines in the development of tumors and the

potential of annatto-tocotrienol and found that higher serum cytokine (TNF-α and IL-6) levels were detected. The colon tissue exhibited infiltration of lymphocyte. Additionally, we observed decreased serum cytokine levels, including IL-4 and IL-10. These observations suggest that these cytokines are implicated in the tumorigenesis of AOM/DSS-induced colon tumors in mice. Treatment with annatto-tocotrienol significantly reduced the levels of inflammatory cytokines in the serum of CAC mice, and inhibited the infiltration of the immune cells in the CAC mice colon. In conclusion, annatto-tocotrienol displays anti-inflammation and anti-tumorigenic activity by modulating inflammation-related immune cells and cytokines, and TLRs/MyD88 signaling pathway plays a critical role in CAC development. However, given the AOM/DSS-induced tumor model, it is essential to investigate the anti-tumorigenic effects of annatto-tocotrienol in clinical studies.

CRediT authorship contribution statement

Qian Li: Methodology, Project administration, Investigation, Formal analysis, Writing – original draft. **Shujing Zhang:** Methodology, Project administration, Investigation, Formal analysis, Writing – original draft. **Qinghong Zhou:** Investigation, Resources, Visualization, Software, Writing – original draft. **Chenxi Gu:** Investigation, Data curation. **Yinghua Liu:** Investigation, Resources. **Jing Zhang:** Investigation, Data curation. **Jingshu Zhang:** Conceptualization, Writing – review & editing.

Declaration of competing interest

The authors declare that they have no known competing financial interests or personal relationships that could have appeared to influence the work reported in this paper.

Data availability

Data will be made available on request.

Acknowledgments

The study was funded by the National Natural Science Foundation of China (grant number 81472968), Shandong medical and health science and technology development plan project (grant number 2019WS297) and Tianjin Applied Basic Research Diversified Investment Youth Project (Screening and Mechanism Study of Colorectal Cancer Biomarkers Based on Transcriptomics) (No. 21JCQNJC01810). The authors acknowledge the American River Nutrition, Inc. for supplying the annatto-tocotrienol samples.

References

Abdullah, M., Rani, A.A., Sudoyo, A.W., Makmun, D., Handjari, D.R., Hernowo, B.S., 2013. Expression of NF-kB and COX2 in colorectal cancer among native Indonesians: the role of inflammation in colorectal carcinogenesis. Acta Med. Indones. 45, 187–192.

Akira, S., Takeda, K., Kaisho, T., 2001. Toll-like receptors: critical proteins linking innate and acquired immunity. Nat. Immunol. 2, 675–680. https://doi.org/10.1038/90609.

Angevin, E., Tabernero, J., Elez, E., Cohen, S.J., Bahleda, R., van Laethem, J.-L., Ottensmeier, C., Lopez-Martin, J.A., Clive, S., Joly, F., Ray-Coquard, I., Dirix, L., Machiels, J.-P., Steven, N., Reddy, M., Hall, B., Puchalski, T.A., Bandekar, R., van de Velde, H., Tromp, B., Vermeulen, J., Kurzrock, R., 2014. A phase I/II, multiple-dose, dose-escalation study of siltuximab, an anti-interleukin-6 monoclonal antibody, patients with advanced solid tumors. Clin. Cancer Res. 20, 2192–2204. https://doi.org/10.1158/1078-0432.CCR-13-2200.

Bray, F., Laversanne, M., Sung, H., Ferlay, J., Siegel, R.L., Soerjomataram, I., Jemal, A., 2024. Global cancer statistics 2022: GLOBOCAN estimates of incidence and mortality worldwide for 36 cancers in 185 countries. CA Cancer J. Clin. 74, 229–263. https://doi.org/10.3322/caac.21834.

Brown, M.A., Hural, J., 2017. Functions of IL-4 and control of its expression. Crit. Rev. Immunol. 37, 181–212. https://doi.org/10.1615/CritRevImmunol.v37.i2-6.30.

Codeluppi, S., Fernandez-Zafra, T., Sandor, K., Kjell, J., Liu, Q., Abrams, M., Olson, L., Gray, N.S., Svensson, C.I., Uhlén, P., 2014. Interleukin-6 secretion by astrocytes is dynamically regulated by PI3K-mTOR-calcium signaling. PLoS One 9, e92649.

De Silva, L., Chuah, L.H., Meganathan, P., Fu, J.-Y., 2016. Tocotrienol and cancer metastasis. Biofactors 42, 149–162. https://doi.org/10.1002/biof.1259.

Deng, L., Wang, C., Spencer, E., Yang, L., Braun, A., You, J., Slaughter, C., Pickart, C., Chen, Z.J., 2000. Activation of the IkappaB kinase complex by TRAF6 requires a dimeric ubiquitin-conjugating enzyme complex and a unique polyubiquitin chain. Cell 103, 351–361. https://doi.org/10.1016/s0092-8674(00)00126-4.

Di Martino, L., Dave, M., Menghini, P., Xin, W., Arseneau, K.O., Pizarro, T.T., Cominelli, F., 2016. Protective role for TWEAK/Fn14 in regulating acute intestinal inflammation and colitis-associated tumorigenesis. Cancer Res. 76, 6533–6542. https://doi.org/10.1158/0008-5472.CAN-16-0400.

Dunne, A., O'Neill, L.A.J., 2003. The interleukin-1 receptor/toll-like receptor superfamily: signal transduction during inflammation and host defense. Science's STKE 2003. https://doi.org/10.1126/stke.2003.171.re3.

Fonseca-Camarillo, G., Furuzawa-Carballeda, J., Iturriaga-Goyon, E., Yamamoto-Furusho, J.K., 2018. Differential expression of IL-36 family members and IL-38 by immune and nonimmune cells in patients with active inflammatory bowel disease. Biomed Res. Int. 2018, 1–12. https://doi.org/10.1155/2018/5140691.

Fukata, M., Hernandez, Y., Conduah, D., Cohen, J., Chen, A., Breglio, K., Goo, T., Hsu, D., Xu, R., Abreu, M.T., 2009. Innate immune signaling by Toll-like receptor-4 (TLR4) shapes the inflammatory microenvironment in colitis-associated tumors. Inflamm. Bowel Dis. 15, 997–1006. https://doi.org/10.1002/ibd.20880.

Fukata, M., Shang, L., Santaolalla, R., Sotolongo, J., Pastorini, C., España, C., Ungaro, R., Harpaz, N., Cooper, H.S., Elson, G., Kosco-Vilbois, M., Zaias, J., Perez, M.T., Mayer, L., Vamadevan, A.S., Lira, S.A., Abreu, M.T., 2011. Constitutive activation of epithelial TLR4 augments inflammatory responses to mucosal injury and drives colitis-associated tumorigenesis. Inflamm. Bowel Dis. 17, 1464–1473. https://doi.org/10.1002/ibd.21527.

Garcia Rodriguez, L.A., Cea-Soriano, L., Tacconelli, S., Patrignani, P., 2013:. Coxibs: Pharmacology, Toxicity and Efficacy in Cancer Clinical Trials 67–93. https://doi.org/10.1007/978-3-642-30331-9_4.

Harvanová, G., Duranková, S., Bernasovská, J., 2023. The role of cytokines and chemokines in the inflammatory response. Alergologia Polska - Polish Journal of Allergology 10, 210–219. https://doi.org/10.5114/pja.2023.131708.

Hausmann, M., Kiessling, S., Mestermann, S., Webb, G., Spöttl, T., Andus, T., Schölmerich, J., Herfarth, H., Ray, K., Falk, W., Rogler, G., 2002. Toll-like receptors 2 and 4 are up-regulated during intestinal inflammation. Gastroenterology 122, 1987–2000. https://doi.org/10.1053/gast.2002.33662.

He, W., Liu, Q., Wang, L., Chen, W., Li, N., Cao, X., 2007. TLR4 signaling promotes immune escape of human lung cancer cells by inducing immunosuppressive cytokines and apoptosis resistance. Mol. Immunol. 44, 2850–2859. https://doi.org/10.1016/j.molimm.2007.01.022.

Hirano, T., Hirayama, D., Wagatsuma, K., Yamakawa, T., Yokoyama, Y., Nakase, H., 2020. Immunological mechanisms in inflammation-associated colon carcinogenesis. Int. J. Mol. Sci. 21, 3062. https://doi.org/10.3390/ijms21093062.

Huang, H.-Y., Zhang, Z.-J., Cao, C.-B., Wang, N., Liu, F.-F., Peng, J.-Q., Ren, X.-J., Qian, J., 2014. The TLR4/NF-κB signaling pathway mediates the growth of colon cancer. Eur. Rev. Med. Pharmacol. Sci. 18, 3834–3843.

Hurtubise, R., Audiger, C., Dominguez-Punaro, M.C., Chabot-Roy, G., Chognard, G., Raymond-Marchand, L., Coderre, L., Chemtob, S., Michnick, S.W., Rioux, J.D., Lesage, S., 2019. Induced and spontaneous colitis mouse models reveal complex interactions between IL-10 and IL-12/IL-23 pathways. Cytokine 121, 154738. https://doi.org/10.1016/j.cyto.2019.154738.

Husain, K., Zhang, A., Shivers, S., Davis-Yadley, A., Coppola, D., Yang, C.S., Malafa, M.P., 2019. Chemoprevention of azoxymethane-induced colon carcinogenesis by delta-tocotrienol. Cancer Prev. Res. (Phila.) 12, 357–366. https://doi.org/10.1158/1940-6207.CAPR-18-0290.

Indaram, A.V.K., Visvalingam, V., Locke, M., Bank, S., 2000. Mucosal cytokine production in radiation-induced proctosigmoiditis compared with inflammatory bowel disease. Am. J. Gastroenterol. 95, 1221–1225. https://doi.org/10.1111/j.1572-0241.2000.02013.x.

Jiang, Q., Yin, X., Lill, M.A., Danielson, M.L., Freiser, H., Huang, J., 2008. Long-chain carboxychromanols, metabolites of vitamin E, are potent inhibitors of cyclooxygenases. In: Proceedings of the National Academy of Sciences, pp. 20464–20469. https://doi.org/10.1073/pnas.0810962106.

Katz, Y., Nadiv, O., Rapoport, M.J., Loos, M., 2001. IL-17 regulates gene expression and protein synthesis of the complement system, C3 and factor B, in skin fibroblasts. Clin. Exp. Immunol. 120, 22–29. https://doi.org/10.1046/j.1365-2249.2000.01199.x.

Leulier, F., Lemaitre, B., 2008. Toll-like receptors — taking an evolutionary approach. Nat. Rev. Genet. 9, 165–178. https://doi.org/10.1038/nrg2303.

Li, T., Li, F., Liu, X., Liu, J., Li, D., 2019. Synergistic anti-inflammatory effects of quercetin and catechin via inhibiting activation of TLR4–MyD88-mediated NF-κB and MAPK signaling pathways. Phytother. Res. 33, 756–767. https://doi.org/10.1002/ptr.6268.

Li, Y., Sun, W.-G., Liu, H.-K., Qi, G.-Y., Wang, Q., Sun, X.-R., Chen, B.-Q., Liu, J.-R., 2011. γ-Tocotrienol inhibits angiogenesis of human umbilical vein endothelial cell induced by cancer cell. J. Nutr. Biochem. 22, 1127–1136. https://doi.org/10.1016/j.jnutbio.2010.09.012.

Liu, S., Jia, H., Hou, S., Xin, T., Guo, X., Zhang, G., Gao, X., Li, M., Zhu, W., Zhu, H., 2018. Recombinant Mtb9.8 of Mycobacterium bovis stimulates TNF-α and IL-1β secretion by RAW264.7 macrophages through activation of NF-κB pathway via TLR2. Sci. Rep. 8, 1928. https://doi.org/10.1038/s41598-018-20433-x.

Luan, H., Zhang, Q., Wang, L., Wang, C., Zhang, M., Xu, X., Zhou, H., Li, X., Xu, Q., He, F., Yuan, J., Lv, Y., 2014. OM85-BV induced the productions of IL-1β, IL-6, and

TNF-α via TLR4- and TLR2-mediated ERK1/2/NF-κB pathway in RAW264.7 cells. J. Interferon Cytokine Res. 34, 526–536. https://doi.org/10.1089/jir.2013.0077.
Mittal, R.D., Bid, H.K., Ghoshal, U.C., 2005. IL-1 receptor antagonist (IL-1Ra) gene polymorphism in patients with inflammatory bowel disease in India. Scand. J. Gastroenterol. 40, 827–831. https://doi.org/10.1080/00365520510015629.
Mohd Zaffarin, A.S., Ng, S.-F., Ng, M.H., Hassan, H., Alias, E., 2020. Pharmacology and pharmacokinetics of vitamin E: nanoformulations to enhance bioavailability. Int. J. Nanomed. 15, 9961–9974. https://doi.org/10.2147/IJN.S276355.
Munkholm, P., 2003. Review article: the incidence and prevalence of colorectal cancer in inflammatory bowel disease. Aliment. Pharmacol. Ther. 18, 1–5. https://doi.org/10.1046/j.1365-2036.18.s2.2.x.
Murthy, S.K., Kuenzig, M.E., Windsor, J.W., Matthews, P., Tandon, P., Benchimol, E.I., Bernstein, C.N., Bitton, A., Coward, S., Jones, J.L., Kaplan, G.G., Lee, K., Targownik, L.E., Peña-Sánchez, J.-N., Rohatinsky, N., Ghandeharian, S., Meka, S., Chis, R.S., Gupta, S., Cheah, E., Davis, T., Weinstein, J., Im, J.H.B., Goddard, Q., Gorospe, J., Loschiavo, J., McQuaid, K., D'Addario, J., Silver, K., Oppenheim, R., Singh, H., 2023. The 2023 impact of inflammatory bowel disease in canada: cancer and IBD. J. Can. Assoc. Gastroenterol. 6 (2023), S83–S96. https://doi.org/10.1093/jcag/gwad006.
Nagasaki, T., Hara, M., Nakanishi, H., Takahashi, H., Sato, M., Takeyama, H., 2014. Interleukin-6 released by colon cancer-associated fibroblasts is critical for tumour angiogenesis: anti-interleukin-6 receptor antibody suppressed angiogenesis and inhibited tumour–stroma interaction. Br. J. Cancer 110, 469–478. https://doi.org/10.1038/bjc.2013.748.
Nagata, K., Nishiyama, C., 2021. IL-10 in mast cell-mediated immune responses: anti-inflammatory and proinflammatory roles. Int. J. Mol. Sci. 22, 4972. https://doi.org/10.3390/ijms22094972.
Neufert, C., Becker, C., Neurath, M.F., 2007. An inducible mouse model of colon carcinogenesis for the analysis of sporadic and inflammation-driven tumor progression. Nat. Protoc. 2, 1998–2004. https://doi.org/10.1038/nprot.2007.279.
Okayasu, I., Ohkusa, T., Kajiura, K., Kanno, J., Sakamoto, S., 1996. Promotion of colorectal neoplasia in experimental murine ulcerative colitis. Gut 39, 87–92. https://doi.org/10.1136/gut.39.1.87.
Pastille, E., Faßnacht, T., Adamczyk, A., 2021. Inhibition of TLR4 signaling impedes tumor growth in colitis-associated colon cancer. Front. Immunol. 12, 669747. https://doi.org/10.3389/fimmu.2021.669747.
Peterson, L.W., Artis, D., 2014. Intestinal epithelial cells: regulators of barrier function and immune homeostasis. Nat. Rev. Immunol. 14, 141–153. https://doi.org/10.1038/nri3608.
Popivanova, B.K., Kitamura, K., Wu, Y., Kondo, T., Kagaya, T., Kaneko, S., Oshima, M., Fujii, C., Mukaida, N., 2008. Blocking TNF-α in mice reduces colorectal carcinogenesis associated with chronic colitis. J. Clin. Investig. https://doi.org/10.1172/JCI32453.
Qian, L.I., Chenxi, G.U., Heng, Q.I.N., Qinglu, W.A.N.G., 2021. Annatto-tocotrienol inhibits nuclear factor (NF)-κB signaling pathway in mice with colitis-associated cancer. Acta Nutrimenta Sinica 43, 463–467.
Ribbons, K.A., Thompson, J.H., Liu, X., Pennline, K., Clark, D.A., Miller, M.J.S., 1997. Anti-inflammatory properties of interleukin-10 administration in hapten-induced colitis. Eur. J. Pharmacol. 323, 245–254. https://doi.org/10.1016/S0014-2999(97)00017-4.
Rostom, A., Dubé, C., Lewin, G., Tsertsvadze, A., Barrowman, N., Code, C., Sampson, M., Moher, D., 2007. Nonsteroidal Anti-inflammatory drugs and cyclooxygenase-2 inhibitors for primary prevention of colorectal cancer: a systematic review prepared for the U.S. Preventive Services Task Force, Ann Intern Med 146 376. https://doi.org/10.7326/0003-4819-146-5-200703060-00010.
S. Rutz, W. Ouyang, regulation of interleukin-10 expression, in: 2016: pp. 89–116. https://doi.org/10.1007/978-94-024-0921-5_5.
Saleh, M., Trinchieri, G., 2011. Innate immune mechanisms of colitis and colitis-associated colorectal cancer. Nat. Rev. Immunol. 11, 9–20. https://doi.org/10.1038/nri2891.
Santiago, L., Castro, M., Pardo, J., Arias, M., Mouse model of colitis-associated colorectal cancer (CAC): isolation and characterization of mucosal-associated lymphoid cells, in: 2019: pp. 189–202. https://doi.org/10.1007/978-1-4939-8885-3_13.
Scotti, G.B., Iannone, I., de Padua, C., Crocetti, D., Fiori, G., Sapienza, P., Fiori, E., Avenia, S., Lamazza, A., 2014. Occurrence of colorectal cancer after a negative colonoscopy in patients with inflammatory bowel disease: a systematic review and meta-analysis, in vivo (Brooklyn) 38 (2024) 523–530. https://doi.org/10.21873/invivo.13470.
Serebruany, V.L., Malinin, A.I., Eisert, R.M., Sane, D.C., 2004. Risk of bleeding complications with antiplatelet agents: Meta-analysis of 338,191 patients enrolled in 50 randomized controlled trials. Am. J. Hematol. 75, 40–47. https://doi.org/10.1002/ajh.10451.
Sharma, D., Malik, A., Guy, C.S., Karki, R., Vogel, P., Kanneganti, T.-D., 2018. Pyrin inflammasome regulates tight junction integrity to restrict colitis and tumorigenesis. Gastroenterology 154, 948–964.e8. https://doi.org/10.1053/j.gastro.2017.11.276.
Shen, J., Yang, T., Xu, Y., Luo, Y., Zhong, X., Shi, L., Hu, T., Guo, T., Nie, Y., Luo, F., Lin, Q., 2018. δ-Tocotrienol, isolated from rice bran, exerts an anti-inflammatory effect via MAPKs and PPARs signaling pathways in lipopolysaccharide-stimulated macrophages. Int. J. Mol. Sci. 19, 3022. https://doi.org/10.3390/ijms19103022.
Shibata, A., Nakagawa, K., Sookwong, P., Tsuduki, T., Oikawa, S., Miyazawa, T., 2009. delta-Tocotrienol suppresses VEGF induced angiogenesis whereas alpha-tocopherol does not. J. Agric. Food Chem. 57, 8696–8704. https://doi.org/10.1021/jf9012899.
Siegel, R.L., Miller, K.D., Fuchs, H.E., Jemal, A., 2022. Cancer statistics. CA Cancer J. Clin. 72 (2022), 7–33. https://doi.org/10.3322/caac.21708.
Son, H.J., Sohn, S.H., Kim, N., Lee, H.-N., Lee, S.M., Nam, R.H., Park, J.H., Song, C.-H., Shin, E., Na, H.Y., Kim, J.S., Lee, D.H., Surh, Y.-J., 2019. Effect of estradiol in an azoxymethane/dextran sulfate sodium-treated mouse model of colorectal cancer: implication for sex difference in colorectal cancer development. Cancer Res. Treat. 51, 632–648. https://doi.org/10.4143/crt.2018.060.
Sun, B., Xing, K., Qi, C., Yan, K., Xu, Y., 2020. Down-regulation of miR-215 attenuates lipopolysaccharide-induced inflammatory injury in CCD-18co cells by targeting GDF11 through the TLR4/NF-kB and JNK/p38 signaling pathways. Histol. Histopathol. 35, 1473–1481. https://doi.org/10.14670/HH-18-278.
Suzuki, R., Kohno, H., Sugie, S., Tanaka, T., 2004. Sequential observations on the occurrence of preneoplastic and neoplastic lesions in mouse colon treated with azoxymethane and dextran sodium sulfate. Cancer Sci. 95, 721–727. https://doi.org/10.1111/j.1349-7006.2004.tb03252.x.
Suzuki, R., Kohno, H., Sugie, S., Nakagama, H., Tanaka, T., 2005. Strain differences in the susceptibility to azoxymethane and dextran sodium sulfate-induced colon carcinogenesis in mice. Carcinogenesis 27, 162–169. https://doi.org/10.1093/carcin/bgi205.
Szajnik, M., Szczepanski, M.J., Czystowska, M., Elishaev, E., Mandapathil, M., Nowak-Markwitz, E., Spaczynski, M., Whiteside, T.L., 2009. TLR4 signaling induced by lipopolysaccharide or paclitaxel regulates tumor survival and chemoresistance in ovarian cancer. Oncogene 28, 4353–4363. https://doi.org/10.1038/onc.2009.289.
Tanaka, T., Kohno, H., Suzuki, R., Yamada, Y., Sugie, S., Mori, H., 2003. A novel inflammation-related mouse colon carcinogenesis model induced by azoxymethane and dextran sodium sulfate. Cancer Sci. 94, 965–973. https://doi.org/10.1111/j.1349-7006.2003.tb01386.x.
ten Hove, T., The, F.O., Berkhout, M., Bruggeman, J.P., Vyth-Dreese, F.A., Slors, J.F.M., van Deventer, S.J.H., te Velde, A.A., 2004. Expression of CD45RB functionally distinguishes intestinal T lymphocytes in inflammatory bowel disease. J. Leukoc. Biol. 75, 1010–1015. https://doi.org/10.1189/jlb.0803400.
Terzić, J., Grivennikov, S., Karin, E., Karin, M., 2010. Inflammation and colon cancer. Gastroenterology 138, 2101–2114.e5. https://doi.org/10.1053/j.gastro.2010.01.058.
Ullman, T.A., Itzkowitz, S.H., 2011. Intestinal Inflammation and Cancer. Gastroenterology 140, 1807–1816.e1. https://doi.org/10.1053/j.gastro.2011.01.057.
Wang, Y., Jiang, Q., 2013. γ-Tocotrienol inhibits lipopolysaccharide-induced interlukin-6 and granulocyte colony-stimulating factor by suppressing C/EBPβ and NF-κB in macrophages. J. Nutr. Biochem. 24, 1146–1152. https://doi.org/10.1016/j.jnutbio.2012.08.015.
Xiaoping, Xu., Yue, Su., Pan, Y., Shen, M., Liu, D., Liu, Z., Chen, D., Jia, Wu., 2023. The therapeutic effect of phellopterin on colitis-associated cancer and its effects on TLR4/NF-κB pathway and macrophage M2 polarization. Cell. Mol. Biol. 69, 51–57. https://doi.org/10.14715/cmb/2023.69.15.8.
Xie, L., Jiang, F.-C., Zhang, L.-M., He, W.-T., Liu, J.-H., Li, M.-Q., Zhang, X., Xing, S., Guo, H., Zhou, P., 2016. Targeting of MyD88 homodimerization by novel synthetic inhibitor TJ-M2010-5 in preventing colitis-associated colorectal cancer. J. Natl. Cancer Inst. 108, djv364. https://doi.org/10.1093/jnci/djv364.
Xu, W., Du, M., Zhao, Y., Wang, Q., Sun, W., Chen, B., 2012. γ-Tocotrienol inhibits cell viability through suppression of β-catenin/Tcf signaling in human colon carcinoma HT-29 cells. J. Nutr. Biochem. 23, 800–807. https://doi.org/10.1016/j.jnutbio.2011.04.003.
Yang, D.-H., 2015. Recent advances in understanding colorectal cancer and dysplasia related to ulcerative colitis. Korean J. Gastroenterol. 66, 312. https://doi.org/10.4166/kjg.2015.66.6.312.
Yang, C.S., Luo, P., Zeng, Z., Wang, H., Malafa, M., Suh, N., 2020. Vitamin E and cancer prevention: studies with different forms of tocopherols and tocotrienols. Mol. Carcinog. 59, 365–389. https://doi.org/10.1002/mc.23160.
Zhang, J.-S., Li, D.-M., He, N., Liu, Y.-H., Wang, C.-H., Jiang, S.-Q., Chen, B.-Q., Liu, J.-R., 2011. A paraptosis-like cell death induced by δ-tocotrienol in human colon carcinoma SW620 cells is associated with the suppression of the Wnt signaling pathway. Toxicology 285, 8–17. https://doi.org/10.1016/j.tox.2011.03.011.
Zhang, J.-S., Li, D.-M., Ma, Y., He, N., Gu, Q., Wang, F.-S., Jiang, S.-Q., Chen, B.-Q., Liu, J.-R., 2013. γ-Tocotrienol induces paraptosis-like cell death in human colon carcinoma SW620 cells. PLoS One 8, e57779.
Zhang, J.-S., Zhang, S.-J., Li, Q., Liu, Y.-H., He, N., Zhang, J., Zhou, P.-H., Li, M., Guan, T., Liu, J.-R., 2015. Tocotrienol-rich fraction (TRF) suppresses the growth of human colon cancer xenografts in Balb/C nude mice by the Wnt pathway. PLoS One 10, e0122175.
Zhao, X., Wu, H., Zhu, R., Shang, G., Wei, J., Shang, H., Tian, P., Chen, T., Wei, H., 2023. Combination of thalidomide and Clostridium butyricum relieves chemotherapy-induced nausea and vomiting via gut microbiota and vagus nerve activity modulation. Front. Immunol. 14. https://doi.org/10.3389/fimmu.2023.1220165.
Zhu, G., Cheng, Z., Lin, C., Hoffman, R.M., Huang, Y., Singh, S.R., Zheng, W., Yang, S., Ye, J., 2019. MyD88 regulates LPS-INDUCED NF-κB/MAPK cytokines and promotes inflammation and malignancy in colorectal cancer cells. Cancer Genomics Proteomics 16, 409–419. https://doi.org/10.21873/cgp.20145.